Automatic Picking in the Semblance Domain

Wildney W. S. Vieira, Lourenildo W. B. Leite and Fernando S. M. Nunes, UFPA, Brazil

Abstract

The specific goal of this work was to develop a method for automatic velocity picking based on the semblance function as a nonlinear optimization problem. We define the steps of conventional velocity analysis (CVA) for each CMP in the following way: first, stacking velocities are estimated by means of semblance sum along hyperbolic time trajectories producing a map of $S(v_{\mathbf{rms}}, t_0)$; second, manual picking is performed on this semblance map for several stacking time t_0; third, interval velocities, $v_{\mathbf{int}}$, are calculated based on the picked stacking velocities, $v_{\mathbf{rms}}$, to construct an earth velocity time model, that do not require a reference earth model.

The present work is multi-task as:
1. to eliminate the picking step by considering that stacking velocities are based on an interval velocity model;
2. to search for an interval velocity model that best explains the estimated stacking velocities; and
3. the search is automatic, but subject to physical constraints.

Introduction

Many velocity functions can be defined to represent the underground aiming the geological knowledge. Among them, the relationship between interval velocity and stacking velocity plays an important role in CVA. A primary goal in seismic data processing is the determination of both these velocities, and in CVA interval velocities are calculated from the picked stacking velocities on a semblance map using a mathematical model as, for example, the Durbaum-Dix type (Hubral and Krey, 1980).

The classical drawback of the semblance peak-picking is that a visual interpretation of the map is necessary, and it is based on the amplitude and a velocity window of the semblance map, theorectically for all the CMP. The present study proposes the elimitation of the complete manual peak-picking step by seting up a model driven strategy. Therefore, methods of CVA without manual picking stand as an interesting approach.

The restrictions of the present development can be stated as: (1st) limited to 1-D models; (2nd) use of the Durbaum-Dix model for the relation between v_{int} and v_{rms}; (3rd) it does not taken into account lateral variations; and (4th) the structural dips are not taken into account (Koren and Ravve, 2002).

Method

The CVA is performed by manual picking of points to construct a curve of velocity versus time in the semblance map for each individual common mid-point (CMP) section. But, this task carries a strong subjective decision, and it is present in the free and professional software systems. The result of this operation is a time-distance map of seismic velocity based on CMP families, and this map can be used directely for NMO correction and stack, and for time migration (Vieira, 2011).

This work describes the solution and implementation of the velocity analysis as a non-linear optmization problem under a priori information and constraints, as a possibility for diminishing the direct subjective participation of the semblance map interpretation. The result of the optimization is the root-mean square velocity, v_{rms}. This technique was originally described by (Toldi, 1989), that we denominate automatic velocity analysis (AVA), and the basic reference for the implementation was based on Press et al., (2002), and the process steps are shown in Figure 1.

The optimization realized in the semblance domain was based on two methods:
1. Global Search using the Simplex method;
2. Local Search based on the Conjugate Gradient method.

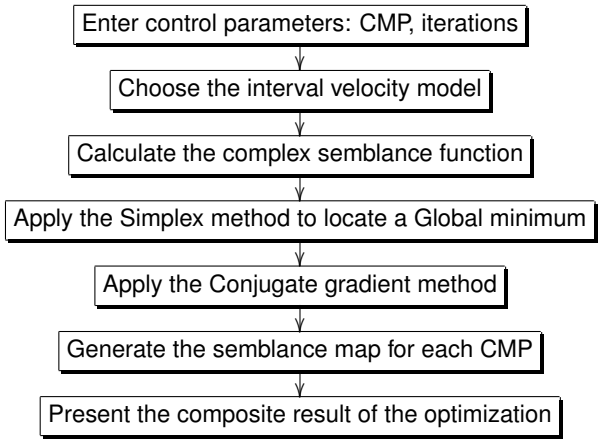

Figure 1: Flowchart of the optimization process.

Simplex Method

This method is based on four basic operations: reflection, expansion, contraction and reduction. It is admited that $\mathbf{x}_i^{(k)}$ be the i-th vertice of the polyhedron in the k-th optimization iteration in the parameter domain $\mathbf{x}$. The correspondent value of the object function of optimization is $f(\mathbf{x}_i^{(k)})$, and

the following definitions are applied:

The $\mathbf{x}_h^{(k)}$ vertice is associated with the largest value of the object function, such that:

$$f(\mathbf{x}_h^{(k)}) = max\left[f(\mathbf{x}_1^{(k)}),\ldots,f(\mathbf{x}_{n+1}^{(k)})\right].$$

The $\mathbf{x}_s^{(k)}$ vertice is associated to the second largest value of the funtion, such that:

$$f(\mathbf{x}_s^{(k)}) = max\left[f(\mathbf{x}_i^{(k)})\right], \quad \forall \quad i \neq h.$$

The $\mathbf{x}_l^{(k)}$ vertice is associated with the smallest value of the object function, such that:

$$f(\mathbf{x}_l^{(k)}) = min\left[f(\mathbf{x}_1^{(k)}),\ldots,f(\mathbf{x}_{n+1}^{(k)})\right].$$

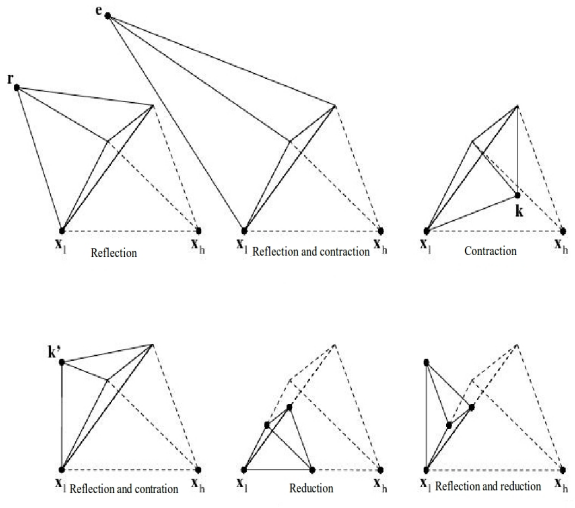

Figure 2: Possible flexible polyhedron transformations for three parameters. The traced lines represent the result of the previous process iteration with respect to the actual.

The initial polyhedron process has for randomly vertices $\mathbf{x}_i^{(0)}$, and at each iteration the vertices $\mathbf{x}_h^{(k)}, \mathbf{x}_s^{(k)}$ and $\mathbf{x}_l^{(k)}$ are determined. For the basic reflection, expansion and contraction operations the centroid is calculated by:

$$\mathbf{c}^{(k)} = \frac{1}{n}\left[\left(\sum_{i=1}^{n+1}\mathbf{x}_i^{(k)}\right) - \mathbf{x}_h^{(k)}\right].$$

The first operation is to reflect the vertice $\mathbf{x}_h^{(k)}$ over the centroid $\mathbf{c}^{(k)}$ to obtain the new vertice in the form:

$$\mathbf{r}^{(k)} = \mathbf{c}^{(k)} + a\left(\mathbf{c}^{(k)} - \mathbf{x}_h^{(k)}\right), \quad \text{with} \quad a > 0.$$

If $f(\mathbf{r}^{(k)}) \leq f(\mathbf{x}_s^{(k)})$, the minimum is expected in the reflection direction. If $f(\mathbf{r}^{(k)}) \leq f(\mathbf{x}_l^{(k)})$, the algorithm tries to acelerate in this direction by means of a reflection:

$$\mathbf{e}^{(k)} = \mathbf{c}^{(k)} + b\left(\mathbf{c}^{(k)} - \mathbf{x}_h^{(k)}\right), \quad \text{with} \quad b > 1.$$

This expanded vertice is accepted if it produces a lower value for $\mathbf{x}_l^{(k)}$. In this way, two possible operations are produced:

Reflection and expansion: $\mathbf{x}_m^{(k)} = \mathbf{e}^{(k)}$, if

$$f(\mathbf{r}^{(k)}) \leq f(\mathbf{x}_l^{(k)}) \wedge f(\mathbf{e}^{(k)}) \leq f(\mathbf{x}_l^{(k)}).$$

Reflection: $\mathbf{x}_m^{(k)} = \mathbf{r}^{(k)}$, if

$$f(\mathbf{x}_l^{(k)}) < f(\mathbf{r}^{(k)}) \leq f(\mathbf{x}_s^{(k)}) \wedge f(\mathbf{e}^{(k)}) > f(\mathbf{x}_l^{(k)}).$$

The reflection is accepted as an intermediary vertice; i.e., $\mathbf{x}_h^{(k)} = \mathbf{f}^{(k)}$, if

$$f(\mathbf{r}^{(k)}) \geq f(\mathbf{x}_h^{(k)}).$$

The next operation is the polyhedron contraction according to:

$$\mathbf{k}^{(k)} = \mathbf{c}^{(k)} + c\left(\mathbf{x}_h^{(k)} - \mathbf{c}^{(k)}\right), \quad \text{with} \quad 0 < c < 1,$$

that is accepted if, $f(\mathbf{k}^{(k)} \leq f(\mathbf{x}_h^{(k)})$.

The transformations are shown in Figure 2 for a three dimensional parameter space ($M = 3$), with the coefficients $a = 1$ for reflection, $b = 2$ for expansion, and $c = \frac{1}{2}$ for contraction.

After each iteration the stop criterion is evaluated, as for instance by:

$$\sqrt{\frac{1}{n+1}\sum_{i=1}^{n+1}\left[f\left(\mathbf{x}_i^{(k)}\right) - f\left(\mathbf{c}^{(k)}\right)\right]^2} \leq \varepsilon, \tag{1}$$

that is the square average of the deviation that form the object calculated with respect to the vertices of the centroid.

Conjugate Gradiente Method

The normalized semblance, $S(v_{\text{rms}}, t_0)$, measures the degree of fitting of amplitudes, $\overline{u}$, of the traces of a CMP family for a certain stack velocity, from a first, $x = x_F$, to a last, $x = x_L$, offset with N_x points, in a temporal window δ, for a certain reflector n, relative to a reference point $P_0(x_0, t_0)$:

$$S(v_{\text{rms}}, t_0) = \frac{\left[\frac{1}{N_t}\sum_{t=t_0-\delta/2}^{t_0+\delta/2}\frac{1}{N_x}\sum_{x=x_F}^{x_L}\overline{u}(x,t_0;v_{\text{rms}})\right]^2}{\frac{1}{N_t}\sum_{t=t_0-\delta/2}^{t_0+\delta/2}\frac{1}{N_x}\sum_{x=x_F}^{x_L}[\overline{u}(x,t_0;v_{\text{rms}})]^2}. \tag{2}$$

$S(v_{\text{rms}}, t_0)$ admits values in the interval $[0,1]$ irrespective of the signal amplitude, and it quantifies the signal polarity uniformity throughout the traces of the corrected NMO family amplitudes $\overline{u}(x,t_0;v_{\text{rms}})$. $S(v_{\text{rms}}, t_0)$ is proportional to the energy ration between numerator and denominator of equation (2). In the NMO correction and stack, the function $S(v_{\text{rms}}, t_0)$ can also be interpreted as a function to be optimized, from where results the optimum value of v_{rms}, where $t(x;t_0,v_{\text{rms}})$ is given by:

$$t(x;t_0,v_{\text{rms}}) = \sqrt{t_0^2 + \frac{x^2}{v_{\text{rms}}^2}}. \tag{3}$$

The Durbaum-Dix transform calculates, for an n-th layer, an interval velocity, v_{int}, from a velocity v_{rms}, in the condition of zero offset:

$$v^2_{\text{int},n} = \frac{t_{n+1}v^2_{\text{rms},n+1} - t_n v^2_{\text{rms},n}}{t_{n+1} - t_n}, \tag{4}$$

or the correspondent velocity v_{rms}, from the interval velocity, v_{int}, is given by:

$$v^2_{\text{rms},n} = \frac{\sum_{i=1}^{n} v^2_{int,i}\Delta t_i}{\sum_{i=1}^{n} \Delta t_i}. \tag{5}$$

The object function of minimization, $Q(\mathbf{m})$, is defined from the semblance function, equation (2), for the entire section, where $\mathbf{m}$ is the velocity vector to be determined:

$$Q(\mathbf{m}) = \sum_{i=1}^{n} S_i(\mathbf{m}). \tag{6}$$

The essential parts of the optimization conjugate gradiente method are described below.

The object function of minimization is $Q(\mathbf{m})$, where $\mathbf{m}$ is the interval velocity vector, $v_{int,i}$, $(i = 1,n)$ to be determined. The functions are approximated by the Taylor series expansion to second order, with $\nabla = \nabla_{m^{(k)}}$ as the coordinates $\mathbf{m}^{(k)}$ of the operator in the k-th actual iteration:

$$Q(\mathbf{m}) \approx Q(\mathbf{m}^{(k)}) + \nabla^T Q(\mathbf{m}^{(k)})(\mathbf{m} - \mathbf{m}^{(k)}) + \frac{1}{2}(\mathbf{m} - \mathbf{m}^{(k)})^T \nabla^2 Q(\mathbf{m}^{(k)})(\mathbf{m} - \mathbf{m}^{(k)}). \tag{7}$$

The gradient vector is given by:

$$\nabla^T Q(\mathbf{m}^{(k)}) = \left[\frac{\partial Q(\mathbf{m}^{(k)})}{\partial m_1} \frac{\partial Q(\mathbf{m}^{(k)})}{\partial m_2} \cdots \frac{\partial Q(\mathbf{m}^{(k)})}{\partial m_M} \right]^T. \tag{8}$$

$$\mathbf{H}(\mathbf{m}^{(k)}) = \nabla^2 Q(\mathbf{m}^{(k)}) = \begin{bmatrix} \frac{\partial^2 Q(\mathbf{m}^{(k)})}{\partial^2 m_1^2} \cdots & \frac{\partial^2 Q(\mathbf{m}^{(k)})}{\partial m_1 \partial m_M} \\ \vdots & \vdots \\ \frac{\partial^2 Q(\mathbf{m}^{(k)})}{\partial m_M \partial m_1} \cdots & \frac{\partial^2 Q(\mathbf{m}^{(k)})}{\partial^2 m_M} \end{bmatrix}. \tag{9}$$

The conjugate gradiente has the following steps:
Change the maximization to a minimization problem:

$$\underline{Q}(\mathbf{m}) > -Q(\mathbf{m}).$$

Update the parameters from a point $\mathbf{m}^{(k)}$ to $\mathbf{m}^{(k+1)}$ along the direction $\mathbf{s}^{(k)}$ with the factor $\lambda^{*(k)}$, where k is the actual and $k+1$ the next iteration:

$$\mathbf{m}^{(k+1)} = \mathbf{m}^{(k)} + \Delta\mathbf{m}^{(k)} = \mathbf{m}^{(k)} + \lambda^{*(k)}\mathbf{s}^{(k)}. \tag{10}$$

Calculate the direction $\mathbf{s}^{(0)}$ by:

$$\mathbf{s}^{(0)} = -\nabla Q(\mathbf{m}^{(0)}). \tag{11}$$

Calculate the factor $\lambda^{*(0)}$ by:

$$\lambda^{*(0)} = -\frac{1}{||\nabla Q(\mathbf{m}^{(0)})||} \frac{\nabla^T Q(\mathbf{m}^{(0)})\hat{\mathbf{s}}^{(0)}}{(\hat{\mathbf{s}}^{(0)})^T \mathbf{H}\hat{\mathbf{s}}^{(0)}}. \tag{12}$$

The direction $\mathbf{s}^{(i)}$ is said be conjugated to direction $\mathbf{s}^{(j)}$ with respect to a matrix defined positive (square), $\mathbf{S}$, if:

$$(\mathbf{s}^{(i)})^T \mathbf{S}(\mathbf{s}^{(j)}) = 0, \quad \text{for } (0 \le i \ne j \le n-1). \tag{13}$$

Calculate ω_k to make $\mathbf{s}^{(k)}$ and $\mathbf{s}^{(k+1)}$ conjugate with respect to $\mathbf{H}$, that results in the expression:

$$\omega_k = \frac{\nabla^T Q(\mathbf{m}^{(k)})\nabla Q(\mathbf{m}^{(k)})}{\nabla^T Q(\mathbf{m}^{(k-1)})\nabla Q(\mathbf{m}^{(k-1)})}; \tag{14}$$

$$\mathbf{s}^{(k)} = -\nabla Q(\mathbf{m}^{(k)}) + \frac{\nabla^T Q(\mathbf{m}^{(k)})\nabla Q(\mathbf{m}^{(k)})}{\nabla^T Q(\mathbf{m}^{(k-1)})\nabla Q(\mathbf{m}^{(k-1)})}. \tag{15}$$

The j-th gradient component is expressed with the help of the chain rule partial differentiation. The sequence of formulas are as follows:

The object gradient is given by:

$$\nabla_{\mathbf{m}^{(k)}} Q(\mathbf{m}^{(k)}) \Big|_j = \frac{\partial Q(\mathbf{m})}{\partial m_j}\Big|_{\mathbf{m}=\mathbf{m}^{(k)}} = \sum_{i=1}^{n} \frac{\partial S[w(\mathbf{m})]}{\partial w_i} \frac{\partial w_i(\mathbf{m})}{\partial m_j}. \tag{16}$$

The numeric gradient is defined by:

$$\frac{\partial S(\mathbf{m})}{\partial w_i}\Big|_{\mathbf{m}=\mathbf{m}^{(k)}} \approx \frac{S[w_i(\mathbf{m}) + \Delta w_i] - S[w_i(\mathbf{m})]}{\Delta w_i}. \tag{17}$$

The parametrized gradient is given by :

$$\frac{\partial w_i(\mathbf{m})}{\partial m_j}\Big|_{\mathbf{m}=\mathbf{m}^{(k)}} = \frac{t_{0,j} - t_{0,j-1}}{t_{0,i}} \left[\frac{w(\mathbf{m}^{(k)})}{m_j} \right]^3, \quad (\text{for } j \le i); \tag{18}$$

$$= \frac{\partial w_i(\mathbf{m})}{\partial m_j}\Big|_{\mathbf{m}=\mathbf{m}^{(k)}} = 0, \quad (\text{for } j > i). \tag{19}$$

The derivative in equation (19) is zero for $j > i$ because the stack velocity at $t_{0,i}$ is not affected by changes in the interval velocities of the deeper layers. Each derivative $\partial w_i(\mathbf{m})/\partial m_j$ is a component of the matrix $\mathbf{G}$, where the elements along the lines, i, are the velocities v_{rms}, and along the columns, j, are the parameters, and:

$$\mathsf{G}_{i,j} = \frac{\partial w_i(\mathbf{m})}{\partial m_j}\Big|_{\mathbf{m}=\mathbf{m}^{(k)}}. \tag{20}$$

The form of the gradient matrix gradiente for the object function is given by:

$$\nabla_{\mathbf{m}^{(k)}} Q(\mathbf{m}^{(k)}) \Big|_j = \sum_{i=1}^{n} \frac{\partial S[w(\mathbf{m})]}{\partial w_i} \mathsf{G}_{i,j}\Big|_{\mathbf{m}=\mathbf{m}^{(k)}}; \tag{21}$$

and the compact form is given by:

$$\nabla_{\mathbf{m}} Q(\mathbf{m})|_{\mathbf{m}^{(k)}} = \mathbf{G}^T \nabla_w S(\mathbf{m})|_{\mathbf{m}^{(k)}}. \tag{22}$$

The linear approximation for the velocity $w(\mathbf{m})$ is given by:

$$w(\mathbf{m}^{(k+1)}) \approx w(\mathbf{m}^{(k)}) + \mathbf{G}\Delta\mathbf{m}. \tag{23}$$

Complex Coherency Functionals

The coherency functional used follows the description of Bernabini et al.(1981) for the case of complex-valued gathers as:

$$\psi(x,t) = p(x,t) + \mathbf{i}q(x,t); \tag{24}$$

where $p(x,t)$ is an usual real-valued gather, and $q(x,t)$ is obtained from $p(x,t)$ by application of the Hilbert transform with respect to time t, i.e.,

$$q(x,t) = \mathbf{H}\{p(x,t)\} = \mathbf{F}^{-1}\{\boldsymbol{i}\mathrm{sgn}(\omega)\}\mathbf{F}\{p(x,t)\}, \tag{25}$$

where $\mathbf{F}$ and $\mathbf{F}^{-1}$ represent the direct and the inverse Fourier transform, respectively, $\mathbf{i}$ is the imaginary unit, and ω is the angular frequency. The semblance functional $\mathscr{S}$ generalizes to:

$$\mathscr{S}(v,t_0) = \frac{\sum_{t=t_0-\delta t/2}^{t_0+\delta/2} \left| \frac{1}{N_x} \sum_{x=x_0}^{X} \psi(x,t;v) \right|^2}{\sum_{t=t_0-\delta t/2}^{t_0+\delta/2} \frac{1}{N_x} \sum_{x=x_0}^{X} |\psi(x,t;v)|^2}, \tag{26}$$

where the vertical bars denote the moduli of the complex numbers involved, and if it operates on complex-valued ψ the functional, $\mathscr{S}$ is still a real-valued coherency.

Results and Conclusions

Figures 3, 4 and 5 show the selected seismic sections of the Jequitinhonha Basin, where the reflection events can be clearly observed, and that were used in the automatic picking on the semblance function. The v_{rms} a priori information used for the optimization was taken from the CMP 2000. As can be seen, the extrapolation to the left and to the right gave the expected good results. The CMP of number 2000 is the reference CMP to extrapolate the information to the left and to the right. The manual picking was performed intentionally only down to 4.0 seconds.

Figures 6, 7 and 8 show the results of the complex semblance optimization, according to equation (26), where the $t_0 - v_{\text{rms}}$ picking can be seen, and this figure was generated using the velocity interval $dv = 10$m/s.

Figure 9 shows in blue line the initial interval velocity, v_{int}, obtained from the v_{rms} velocity picked on the semblance map, and presented for comparison. The red line represents the random inferior and superior limits of the interval velocity, v_{int}, for the Simplex method for the Global Search in the time section. The green line represents the v_{rms} velocity that shows a much smoother aspect than the intervalar velocity v_{int}.

Figures 10, 11 and 12 of the complex semblance show superposition of the root-mean-square velocity in the complex semblance map on the section.

The following conclusions stand from the results. The experiments show that inverting from interval velocities, v_{int}, the solution converges to the v_{rms} velocities; therefore, an estimation of v_z velocities can be made.

There is a necessity to edit the interval velocity, v_{int}, solution in order to smooth out jumps in the result, and this is interpreted as a source of noise in the method.

We observed in the experiments the necessity of an initial model that comtemplates the semblance, and offers the semblance an a priori information.

We demonstrated that the extrapolation of the priori information, manully picked v_{rms} on the semblance output, is useful for interpreting the neightboor CMP's.

As a perspective, we can now extrapolate the interpreted CMP's semblance v_{rms} picking for number of cdps posisitioned to the left and to the right of the reference CMP information.

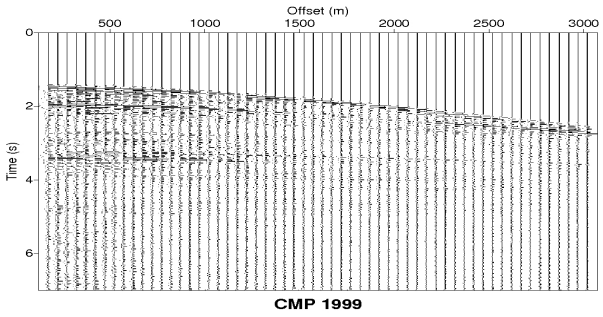

Figure 3: Section CMP 1999 of the Jequitinhonha Basin, where the reflection events can be seen.

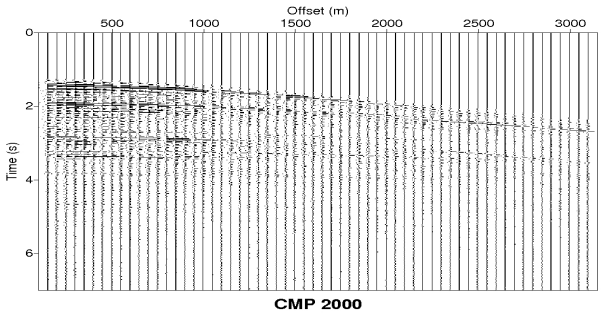

Figure 4: Section CMP 2000 of the Jequitinhonha Basin, where the reflection events can be seen.

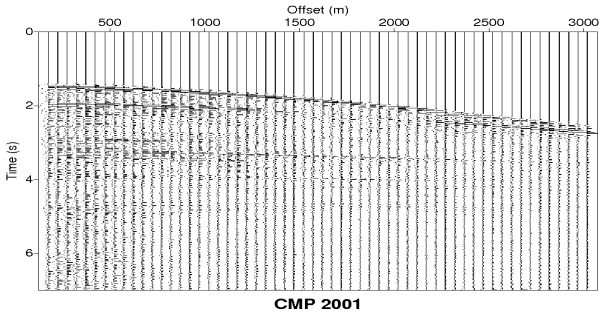

Figure 5: Section CMP 2001 of the Jequitinhonha Basin, where the reflection events can be seen.

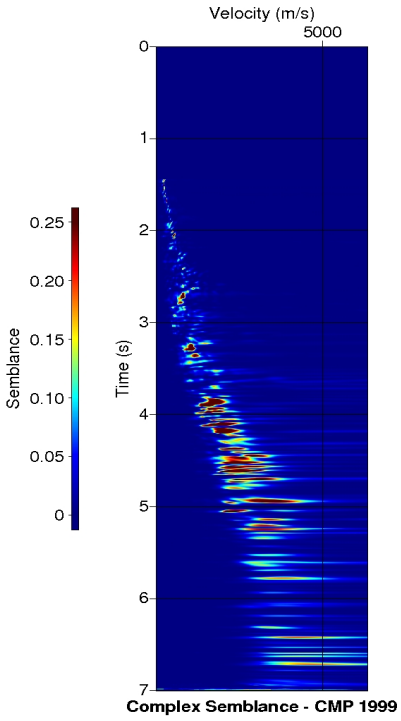

Figure 6: Complex semblance map of section CMP 1999 of the Jequitinhonha Basin.

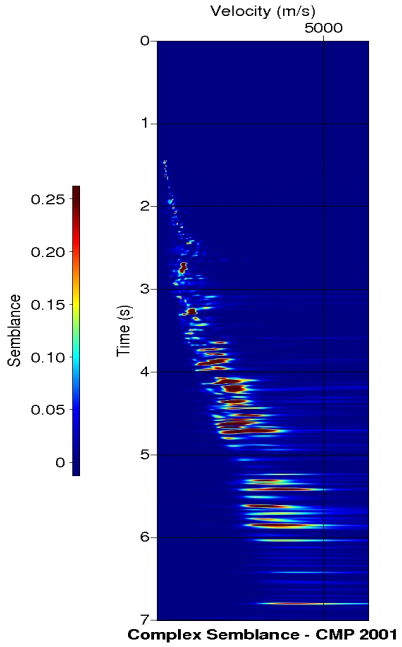

Figure 8: Complex semblance map of section CMP 2001 of the Jequitinhonha Basin.

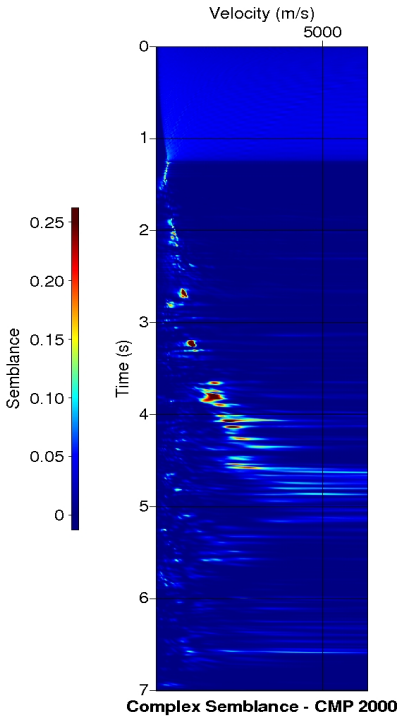

Figure 7: Complex semblance map of section CMP 2000 of the Jequitinhonha Basin.

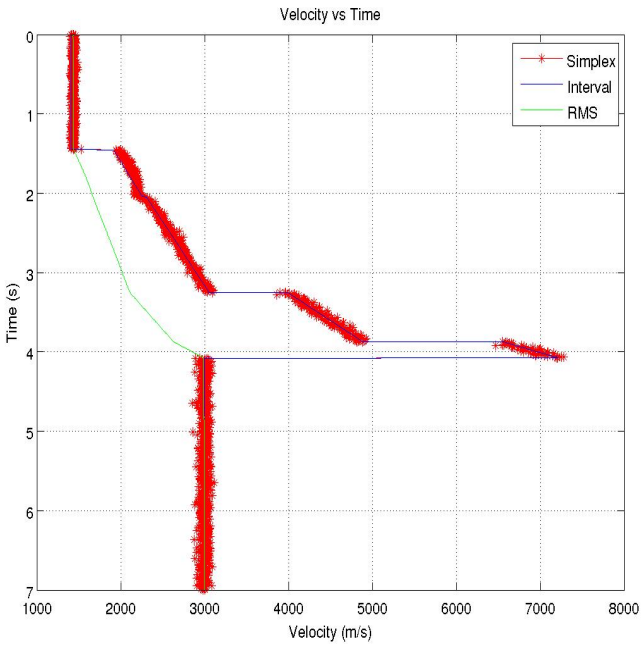

Figure 9: Interval and root-mean-square velocity distributions of section CMP 2000 of the Jequitinhonha Basin showing a good agreement of solutions.

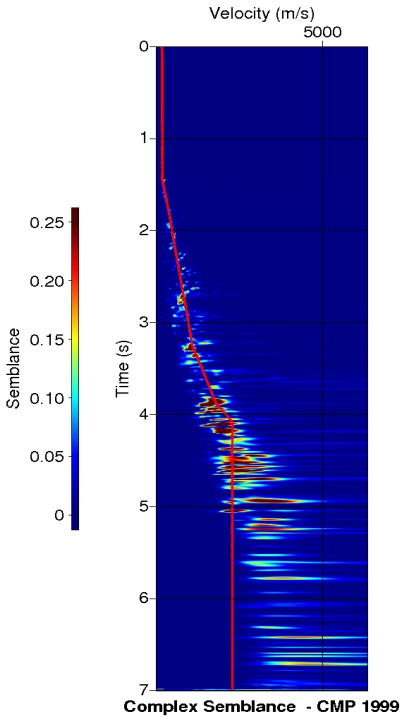

Figure 10: Superposition in the complex semblance map of the root-mean-square velocity on the section CMP 1999. The red curve represents the v_{rms} result.

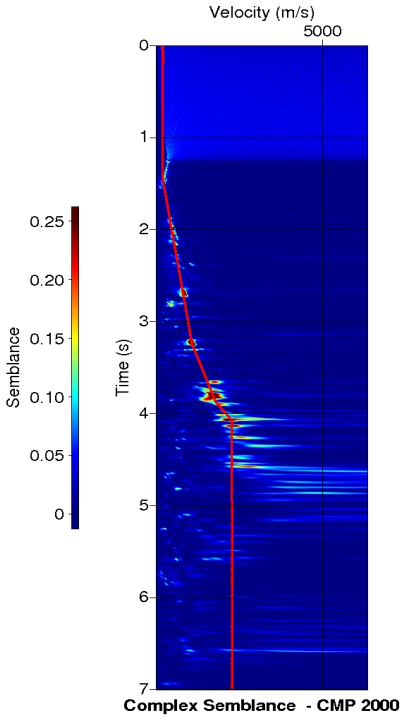

Figure 11: Superposition in the complex semblance map of the root-mean-square velocity on the section CMP 2000. The red curve represents the v_{rms} result.

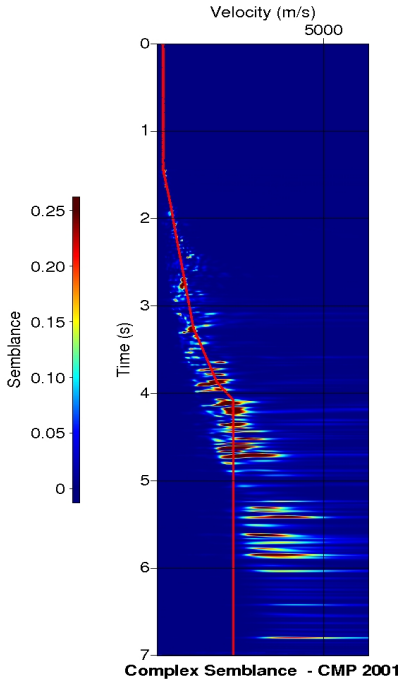

Figure 12: Superposition in the complex semblance map of root-mean-square velocity on the section CMP 2001. The red curve represents the v_{rms} result.

References

Bernabini, M., Carrion, P., Jacovitti, G., Rocca, F. and Treitel, S., 1987, Deconvolution and Inversion: Blackwell Scientific Publications.

Hubral, P. and Krey, T., 1980, Interval Velocities from Seismic Reflection Time Measurements: Society of Exploration Geophysicists.

Koren, Z. and Ravve, I., 2006, Constrained Dix inversion: Geophysics, Vol 7, No. 6, p.113-130.

Press, W. H., Teukolsky, A., Vetterking, W.T. and B. P. Flannery, 2002 , Numerical Recipes in FORTRAN 90: Cambridge University Press, p.227-245.

Toldi, L. T., 1989, Velocity analysis without picking: Geophysics, Vol 54, No. 2, p.191-199.

Vieira, W. W. S., 2011, Velocity Analyis by Optimization by the Semblance in Reflection Seismics: Master Dissertation in Geophysics. Federal University of Pará, Belém, Brazil. (In Portuguese).

Acknowledgments

The authors would like to thank the Brazilian institutions UFPA (*Universidade Federal do Pará*), FINEP (*Financiadora de Estudos e Projetos*), ANP (*Agência Nacional do Petróleo*) and PETROBRAS (*Petróleo Brasileiro S/A*) for the research support, and in special to the National Institute of Science and Technology (*Instituto Nacional de Ciência e tecnologia, INCT-GP, do MCT/CNPq/FINEP*). The thanks are also extended to CAPES for the scholarship.